Journal of Nuclear Materials xxx (2013) xxx–xxx

Contents lists available at SciVerse ScienceDirect

Journal of Nuclear Materials

journal homepage: www.elsevier.com/locate/jnucmat

Response of NSTX liquid lithium divertor to high heat loads

T. Abrams [a,*,1], M.A. Jaworski [a], J. Kallman [b], R. Kaita [a], E.L. Foley [c], T.K. Gray [d], H. Kugel [a], F. Levinton [c], A.G. McLean [b], C.H. Skinner [a]

[a] Princeton Plasma Physics Laboratory, Princeton, NJ 08543, USA
[b] Lawrence Livermore National Laboratory, Livermore, CA 94550, USA
[c] Nova Photonics, Inc., Princeton, NJ 08543, USA
[d] Oak Ridge National Laboratory, Oak Ridge, TN 37831, USA

ARTICLE INFO

Article history:
Available online xxxx

ABSTRACT

Samples of the NSTX Liquid Lithium Divertor (LLD) with and without an evaporative Li coating were directly exposed to a neutral beam *ex-situ* at a power of ~1.5 MW/m^2 for 1–3 s. Measurements of front face and bulk sample temperature were obtained. Predictions of temperature evolution were derived from a 1D heat flux model. No macroscopic damage occurred when the "bare" sample was exposed to the beam but microscopic changes to the surface were observed. The Li-coated sample developed a lithium hydroxide (LiOH) coating, which did not change even when the front face temperature exceeded the pure Li melting point. These results are consistent with the lack of damage to the LLD surface and imply that heating alone may not expose pure liquid Li if the melting point of surface impurities is not exceeded. This suggests that flow and heat are needed for future PFCs requiring a liquid Li surface.

1. Introduction

One of the most prominent issues barring the path to magnetically confined fusion reactors involves developing plasma-facing components (PFCs) that can withstand the high heat and particle fluxes in a reactor environment. Recent experiments with Li-coated PFCs on the National Spherical Torus eXperiment (NSTX) have shown evidence of improved confinement and ELM reduction [1]. The Liquid Lithium Divertor (LLD) was installed on NSTX in 2010 to test the concept of a Li-coated porous Mo surface. While the LLD was intended to provide a Li PFC, there was a concern that the liquid Li could be ejected and expose the Mo substrate [2]. It was thus useful to test the Mo surface as a low-sputtering PFC and the ability of a thin surface layer to allow heat transmission to an underlying copper heat sink.

In situ head load testing of the LLD is difficult due to the complex tokamak environment in which it resides. This motivated off-line heat load testing where heat and particle sources can be carefully controlled and studied. The primary goal of these experiments was to determine if the "bare" LLD surface would experience significant physical damage during NSTX divertor heat loading. The secondary motivation was to quantify any microscopic damage that may result on the porous Mo surface due to plasma bombardment.

Initial experiments were performed using the hydrogen diagnostic neutral beam (DNB) for the Motional Stark Effect Laser Induced Fluorescence (MSE-LIF) diagnostic system [3,4] on NSTX. A small prototype LLD sample was repeatedly bombarded by the DNB at a peak heat flux of ~1.5 MW/m^2. The DNB was used to simulate the high heat and particle fluxes on the LLD itself, which experienced $q_{\perp,peak}$ up to 5 MW/m^2, but only for a small subset of discharges for durations $\leqslant$0.5 s [5]. Subsequent heat loading experiments were performed using a second prototype sample that was coated with a 150 μm Li layer. The primary goal of this experiment was to quantify the effects of high heat flux on a Li-coated Mo substrate. A secondary goal was to examine the extent and effects of Li passivation on the LLD surface.

The temporal and spatial evolution of the surface temperature was monitored using an infrared (IR) camera as well as two embedded thermocouples. A thermal analysis of the IR data was subsequently performed using 1D analytic model to calculate heat fluxes. These calculations were corroborated with calorimetry measurements obtained from thermocouple data. Optical microscopy was performed on both samples at 10× magnification before and after exposure to the DNB, and for the Li-coated sample, before and after cleaning. The resulting images were analyzed with an image-processing algorithm. The primary result presented in this paper is the output of this algorithm: spatially-resolved "damage" profiles which quantify microscopic changes in sample surface morphology due to bombardment by the DNB.

* Corresponding author. Address: PPPL, P.O. Box 451, Princeton, NJ 08543-0451, USA.
E-mail address: tabrams@pppl.gov (T. Abrams).
[1] Presenting author.

0022-3115/$ - see front matter © 2013 Elsevier B.V. All rights reserved.
http://dx.doi.org/10.1016/j.jnucmat.2013.01.057

2. Materials and methods

The LLD and the prototype samples consist of a 152 μm porous molybdenum (Mo) coating plasma-sprayed onto 254 μm of stainless steel, which is in turn explosively bonded to a 1.9 cm copper plate [6]. Each prototype LLD sample measures approximately 3.6 cm by 4.9 cm, yielding a surface area of about 18 cm^2. Two Type K thermocouples were cemented into small wells on the sample: one 2 mm behind the front face and another centered on the rear face.

Two strip heaters were affixed to the bottom face of the Li-coated sample using carbon cement. Approximately 140 mg of 99.9% pure solid Li was placed on the porous Mo surface inside an argon glove box. The temperature of the sample was raised above the 180 °C Li melting point and the Li was allowed to "wick" into the mesh with additional smoothing using a small "scraping" tool. The sample was placed in a sealed argon bag and transported to the DNB test chamber in an adjoining room. Despite efforts to minimize exposure time to full or partial atmosphere, it is believed that the Li layer had developed a lithium hydroxide (LiOH) coating in the period of time between Li application and DNB exposure.

3. Experimental configuration

A diagram of the experimental setup is shown in Fig. 1. The MSE-LIF DNB typically operates a hydrogen beam continuously at 30 kV with 28 mA of plasma current. The prototype sample was mounted on a linear-motion feed-through inside a six-way across approximately 1.5 m from the plasma source. The sample was angled at 45° with respect to the beam line to allow IR measurements to be captured through a 2.5″ ZnSe IR viewport with a transmission efficiency of ≈70%. A far-infrared un-cooled microbolometer Indigo Omega camera provided 1 mm spatial resolution at a sampling rate of 30 Hz in the 8–12 μm wavelength range.

Initial exposures were performed on the "bare" LLD prototype sample. Subsequent exposures were performed on a Li-coated sample. The sample began in the retracted position. The sample was "plunged" down in the path of the neutral beam then quickly retracted after a specified time interval. Roughly 10 exposures were performed that varied in duration from 1 to 3 s. These durations were chosen in order to simulate a series of NSTX discharges that have a typical pulse length of 1 s. During each exposure, temperature measurements were recorded by the IR camera. A false-color image of the sample captured by the camera during beam operation is shown in Fig. 2. Absolute temperatures were determined via an *ex situ* calibration on the bare Mo sample and an additional *in situ* calibration for the Li-coated sample. Front face (the Li/Mo surface) and bulk sample temperatures were also recorded using the two embedded thermocouples.

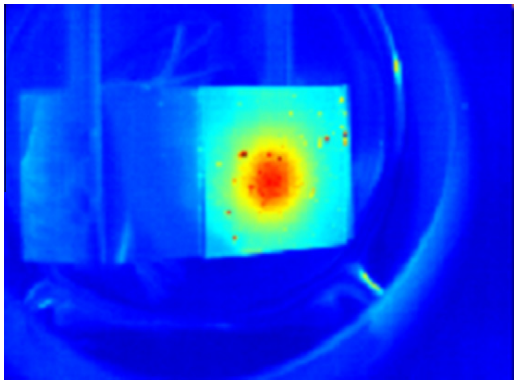

Fig. 2. A false color image of the "bare" LLD sample during neutral beam exposure.

4. Results and discussion

4.1. Thermal analysis of heat flux

The horizontal temperature profile on the sample measured by the IR camera is shown in Fig. 3. Both the horizontal and vertical profiles are assumed to be symmetric along axes extending through the center of the beam line, but are not completely radially symmetric due to the 45° incidence angle of the neutral beam. These profiles are further assumed to follow a Maxwellian distribution and have a calculated half-width at half maximum (HWHM) of 1.5 cm and 1.5*cos(45°) ≈ 1.1 cm, respectively. These parameters, in conjunction with calorimetry calculations using thermocouple data, are sufficient to calculate the net heat flux of the DNB as a function of position on the sample surface. The finite "plunge time" of the sample was compensated for by analyzing the IR data frame-by-frame while the sample was descending and determining the fractional power of the beam deposited onto the sample at each time point. A linear fit to a plot of bulk sample temperature rise to total exposure time produces an average rate of net energy deposition $\langle J \rangle \approx 1.0$ kJ/s. The net heat flux of the beam is thus modeled by:

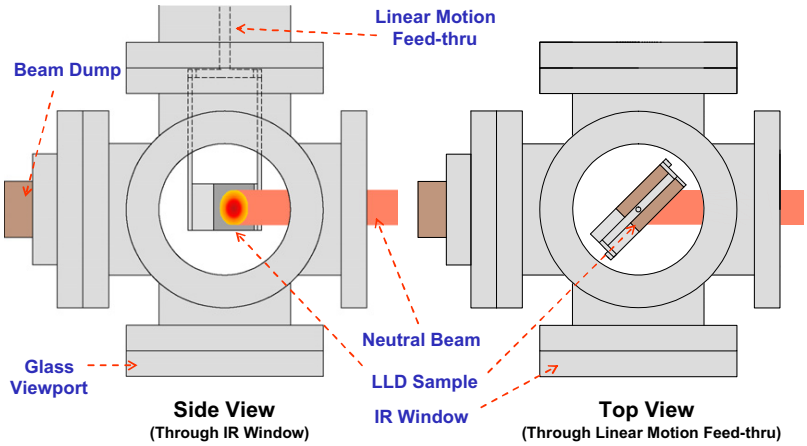

Fig. 1. A view of the experimental apparatus through the IR window mounted on one side of the six-way cross and the linear motion feed-through mounted on top of the cross.

Please cite this article in press as: T. Abrams et al., J. Nucl. Mater. (2013), http://dx.doi.org/10.1016/j.jnucmat.2013.01.057

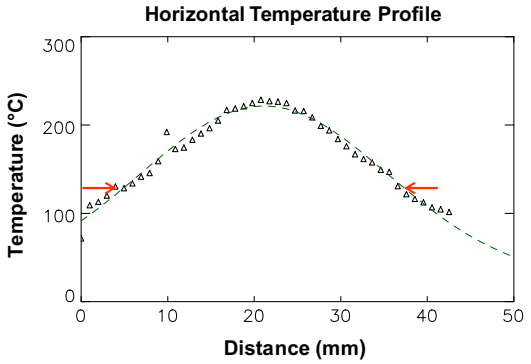

Fig. 3. The horizontal temperature profile on the front face of the LLD sample.

$$q(x,y) = \frac{\langle J \rangle}{2\pi\sigma_x\sigma_y} \exp\left[\frac{-x^2}{2\sigma_x^2} + \frac{-y^2}{2\sigma_y^2}\right] \quad (1)$$

where x and y refer to the horizontal and vertical distance from the center of the beam along the surface of the sample. This calculation yields a peak heat flux $q(0,0)$ of 1.2 MW/m^2.

These calculated heat fluxes were benchmarked against a 1D analytic model which treats the copper bulk as a semi-infinite slab. The porous Mo, stainless steel, and Li layers were treated as thin slabs of finite thickness. The temperature drop across each layer was approximated as $\Delta z/k$, where Δz is the layer thickness and k is thermal conductivity. This approximation is possible because the thermal diffusion time through each of these layers is on the order of several milliseconds. To account for the 50% porosity of the Mo layer, k_{Mo} was multiplied by a factor of 0.5. Using the standard 1D treatment of thermal diffusion [7] and assuming constant heat flux q, one can model the thermal evolution of the sample by:

$$T(t, z=0) = T_0 + q\left[\left(\frac{4\alpha_{Cu}t}{\pi k_{Cu}^2}\right)^{1/2} + \frac{\Delta z_{Mo}}{k_{Mo}} + \frac{\Delta z_{SS}}{k_{SS}} + \frac{\Delta z_{Li}}{k_{Li}}\right] \quad (2)$$

where α_{Cu} is the thermal diffusion coefficient for copper and T_0 is the initial sample temperature in Kelvin. The $\Delta z_{Li}/k_{Li}$ term was omitted during the bare sample analysis.

The thermal evolution of the sample surface measured by the IR camera at the center of the beam for a bare sample exposure is shown in Fig. 4. It was discovered that the temperature rise during the first few milliseconds of the beam exposure (when the thermal response of the Mo and SS layers dominates over the copper) was much faster than the analytic model predicted. Possible explanations for this discrepancy are poor thermal contact between the Mo and SS layers and that the thermal conductivity of porous Mo is substantially lower than $k_{Mo}/2$. Either effect can be modeled by allowing k_{Mo} to vary, introducing an "effective" thermal conductivity. This approach yields a peak heat flux on the sample of 1.5 MW/m^2 and an effective thermal conductivity $k_{eff} = k_{Mo}/20$. An investigation into the origin of this factor of 20 is ongoing.

The heat flux can also be calculated without assuming it is constant in time through numerical methods. A forward in time, centered in space (FTCS) finite-difference scheme [8] was applied to the thermal diffusion equation using the same boundary conditions as the analytic model. T_1^n and T_j^0 are known for all n (time coordinate) and j (spatial coordinate), respectively, on the computational grid. Thus we obtain a well-posed problem with n equations and n unknowns that can be solved for q^n in terms of known values of T_j^n:

$$q^n = \frac{k_{Cu}}{\Delta z}\left\{\left[\frac{T_1^{n+1} - T_1^n}{\Delta t}\right]\frac{(\Delta z)^2}{\alpha_{Cu}} - T_2^n + T_1^n\right\} \quad (3)$$

The time-dependent heat fluxes at the center of the beam obtained with this numerical model are shown in Fig. 5. Note that thin surface layers cannot be incorporated into this model because the algorithm becomes unstable [8] when $\Delta z < (2\alpha\Delta t)^{1/2} \approx 2.7$ mm.

Peak flux estimates obtained from calorimetry, analytic thermal modeling, and numerical thermal modeling lie between 1.0 and 1.5 MW/m^2. As each model relies upon a different set of assumptions the spread in these values is not unexpected.

4.2. Analysis of sample morphology

Each sample was first analyzed via visual inspection to ensure that no gross melting or erosion occurred on the molybdenum surface. Optical microscopy was then performed on both samples using National Instruments Microscope DC3-4201, capable of up to 100× magnification. The images analyzed were captured at 10× magnification, which corresponds to a resolution of approximately 1 μm/pixel. A "panorama" of images was produced by moving the sample in 1–2 mm increments across the Mo surface horizontally through the center of the beam exposure location. This procedure was performed before and after exposure to the DNB for the bare sample and after exposure for the Li-coated sample. Analysis of these images "by eye" before and after particle bombardment indicated no obvious microscopic damage to the "bare" or lithiated porous Mo surface.

These images were analyzed with ImageJ [9] to quantify possible microscopic changes in sample surface morphology. First, each full-color image was converted to 8-bit grayscale. Next, the images

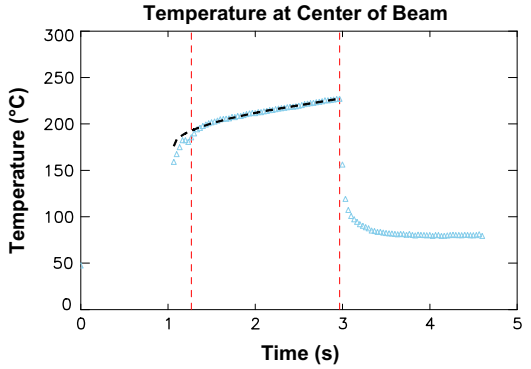

Fig. 4. Thermal evolution of the front face of the bare LLD sample at the center of the beam during a ~1.8 s exposure.

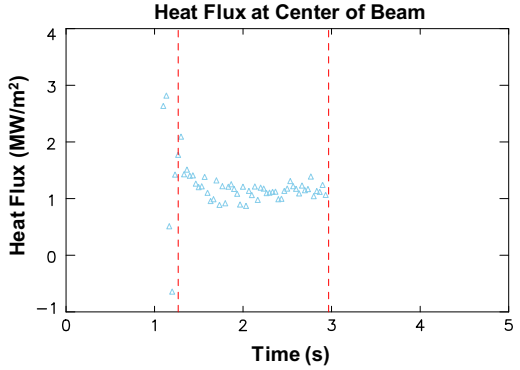

Fig. 5. Heat flux at the center of the beam as determined from a 1-D numerical model.

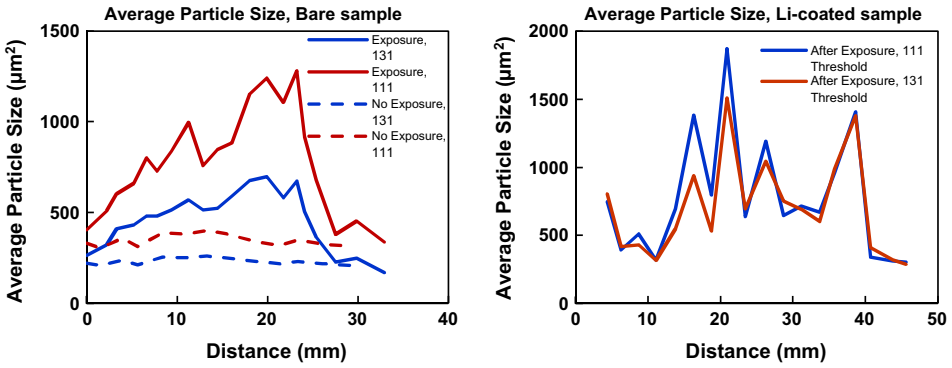

Fig. 6. Average particle size plotted against distance across the surface of the bare sample (left) and Li-coated sample (right).

were converted to black and white using a user-defined "black threshold." Pixels with intensities above this threshold were converted to black while the remaining pixels were converted to white. The two black thresholds used were 111 and 131. The resulting number of black regions on each image was tabulated and divided by the total black area to yield an average "particle size". This average particle size measurement represents a quantitative characterization of the surface morphology captured in each image.

Average particle sizes as a function of position before and after beam exposure are plotted in Fig. 6. The porous Mo layer is nearly uniform in average particle size prior to exposure. A smoothly varying pattern in the surface morphology is evident after beam exposure on the bare LLD sample that correlates with the Gaussian heat flux profile of the beam. The absence of significant macroscopic damage, however, is consistent with effective heat transmission through the thin surface layer to the underlying copper heat sink.

No such smoothly varying morphology pattern, however, is evident on the Li-coated LLD sample surface. This suggests that the surface did not melt during beam exposure tests in excess of 250 °C, which is well above the Li melting point 180 °C. As noted in Section 2, an impurity layer composed of LiOH formed on the lithiated surface. LiOH has a melting point of 462 °C, which was not reached during these experiments.

IR thermography analysis performed in [5] indicates that the plasma-facing surface of the LLD never exceeded 450 °C and typically operated in a temperature range from 200 to 300 °C. In addition, recent laboratory experiments [10,11] have shown that even at the 10^{-8} torr partial pressures of water typically found in tokamaks, a LiOH impurity layer forms on a pure liquid lithium surface within 150–200 s. This implies that during LLD operation in NSTX, a pure liquid lithium surface may not have been exposed to the plasma.

5. Conclusions

Offline experiments at heat fluxes comparable to the NSTX divertor indicate that a layer comprised of Li compounds on the LLD surface will not melt or suffer significant erosion at temperatures in excess of 250 °C. Measurements have shown that a LiOH layer undergoes microscopic changes at this temperature but remains essentially intact. These results also underscore the difficulty of maintaining a pure Li surface under typical tokamak vacuum conditions. This effort is part of an ongoing investigation into the physical and chemical mechanisms behind this passivation process, the goal of which is to form a causal link between tokamak wall conditions and edge plasma behavior.

Acknowledgements

This work is supported by US DOE Contracts DE-AC02-09CH11466 and DE-AC05-00OR22725. Special appreciation is extended to the late John Timberlake for his invaluable assistance in lithium handling.

References

[1] H.W. Kugel et al., J. Nucl. Mater. 415 (2011) S400–S404.
[2] D.G. Whyte et al., Fusion Eng. Des. 72 (2004) 133–147.
[3] E.L. Foley et al., Rev. Sci. Instrum. 77 (2006). 10F311.
[4] E.L. Foley, PhD thesis, Princeton University, 2005.
[5] A.G. McLean et al., J. Nucl. Mater. (2013), http://dx.doi.org/10.1016/j.jnucmat.2013.01.079.
[6] H.W. Kugel et al., Fusion Eng. Des. (2011).
[7] A.F. Mills, Heat and Mass Transfer, CRC Press, 1995.
[8] W.H. Press et al., Numerical Recipes: The Art of Scientific Computing, third ed., Cambridge University Press, New York, 2007.
[9] M.D. Abramoff et al., Biophoton. Int. 11 (7) (2004) 36–42.
[10] C.H. Skinner et al., J. Nucl. Mater. (2013), http://dx.doi.org/10.1016/j.jnucmat.2013.01.136.
[11] R. Sullenberger, MS thesis, Princeton University, 2012.